Observation of Synchrotron Radiation from Electrons Accelerated in a Petawatt-Laser-Generated Plasma Cavity

S. Kneip,[1] S. R. Nagel,[1] C. Bellei,[1] N. Bourgeois,[2] A. E. Dangor,[1] A. Gopal,[3] R. Heathcote,[4] S. P. D. Mangles,[1] J. R. Marquès,[2] A. Maksimchuk,[5] P. M. Nilson,[1] K. Ta Phuoc,[6] S. Reed,[5] M. Tzoufras,[7] F. S. Tsung,[7] L. Willingale,[1] W. B. Mori,[7] A. Rousse,[6] K. Krushelnick,[1,5] and Z. Najmudin[1]

[1]*The Blackett Laboratory, Imperial College London SW7 2AZ, United Kingdom*
[2]*Laboratoire pour l'Utilisation des Lasers Intenses, Ecole Polytechnique, 91128 Palaiseau, France*
[3]*Department of Electronics, Technological Educational Institute of Crete, Romanou, 3-GR73133 Chania, Greece*
[4]*Central Laser Facility, Rutherford Appleton Laboratory, Oxon OX11 0QX, United Kingdom*
[5]*Center for Ultrafast Optical Science (CUOS) University of Michigan, Ann Arbor, Michigan 48109, USA*
[6]*Laboratoire d'Optique Appliqué, ENSTA, Ecole Polytechnique, 91761 Palaiseau, France*
[7]*Department of Physics and Astronomy and Department of Electrical Engineering, UCLA, Los Angeles, California 90095, USA*
(Received 13 December 2007; published 14 March 2008)

The dynamics of plasma electrons in the focus of a petawatt laser beam are studied via measurements of their x-ray synchrotron radiation. With increasing laser intensity, a forward directed beam of x rays extending to 50 keV is observed. The measured x rays are well described in the synchrotron asymptotic limit of electrons oscillating in a plasma channel. The critical energy of the measured synchrotron spectrum is found to scale as the Maxwellian temperature of the simultaneously measured electron spectra. At low laser intensity transverse oscillations are negligible as the electrons are predominantly accelerated axially by the laser generated wakefield. At high laser intensity, electrons are directly accelerated by the laser and enter a highly radiative regime with up to 5% of their energy converted into x rays.

DOI: 10.1103/PhysRevLett.100.105006 PACS numbers: 52.38.Ph, 41.60.Ap, 41.75.Jv, 52.38.Kd

The advent of high power lasers has led to rapid progress in the field of plasma based particle acceleration [1]. In particular, the measurement of monoenergetic electron beams from wakefields generated by short lasers [2] has stimulated great interest in producing such beams and understanding their dynamics. One potential use for these compact sources of energetic particles is as a driver for novel light sources. Laser-accelerated electrons could be injected into a magnetic undulator realizing a compact tunable-energy femtosecond x-ray source synchronized to the laser. A laser-based x-ray source could be downsized further, using the self-generated magnetic and electrostatic fields of the plasma channel as a miniature undulator [3]. For electron beams of sufficiently high quality, an ion channel laser analogous to conventional free electron lasers may be feasible [4]. X rays can also be produced in intense laser-plasma interactions by nonlinear Thomson scattering [5].

Relativistic beams have also been measured from interactions at very high laser intensities, where electrons gain energy directly from the laser [6]. At high intensity, the ponderomotive force of the laser expels plasma electrons, leaving a positively charged ion channel. Electrons inside the channel experience a net focusing force due to the space charge and undergo oscillation at the betatron frequency $\omega_\beta = \omega_p/\sqrt{2\gamma_{z0}}$, where ω_p is the plasma frequency and γ_{z0} is the Lorentz factor associated with the electrons' motion along the plasma channel. Electrons resonant with the laser frequency gain energy from the transverse electric field of the laser, which can be directed into longitudinal momentum through the $\mathbf{v} \times \mathbf{B}$ force [7].

Accelerating charges radiate electromagnetic radiation. For small betatron strength parameters $a_\beta = \gamma_{z0} r_\beta \omega_\beta / c \ll 1$ (undulator limit), the radiation spectrum will be narrowly peaked about the resonant frequency $\omega_1 = M_0 \omega_\beta/(1 + M_0 \alpha^2/2)$ where $2r_\beta$ is the oscillation amplitude, $M_0 = 2\gamma_{z0}^2/(1 + a_\beta^2/2)$ is the Doppler factor, and α is the angle between the direction of observation and the direction of γ_{z0} [8]. This highlights the interdependency of spectral and angular distributions. As $a_\beta \rightarrow 1$, radiation also appears at harmonics of the resonant frequency. For large betatron strength parameter $a_\beta \gg 1$ (wiggler limit), high harmonic radiation is generated and a synchrotron spectrum with broad emission consisting of closely spaced harmonics is produced. The properties of the radiation spectrum for harmonics $m \gg 1$ is given by the synchrotron asymptotic limit (SAL) [8]:

$$\frac{dI}{d(\hbar\omega)} \cong \sqrt{3} \frac{e^2}{\pi \epsilon_0} N_\beta \gamma_{z0} \frac{E}{E_{\text{crit}}} \int_{2\xi}^{\infty} K_{5/3}(\xi') d\xi', \quad (1)$$

N_β is the number of oscillations, $\xi = E/E_{\text{crit}}$, and $E_{\text{crit}} = 3\hbar a_\beta \gamma_{z0}^2 \omega_\beta$ is the energy above and below which roughly half of the total energy is radiated. $K_{5/3}$ is a modified Bessel function of the second kind. The total number of photons, with mean energy of E_{crit}, radiated by N_e electrons, scales as

$$N_{\text{ph}} \propto N_e N_\beta \gamma_{z0}^{1/2} n_e^{1/2} r_\beta, \quad (2)$$

where n_e is the plasma density. The radiation is confined to a cone around $\vec{\beta}$ with opening angle $\theta \approx a_\beta/\gamma_{z0}$.

In this Letter we report the first observation of synchrotron x-ray radiation from relativistic electrons produced from a gas target irradiated with a petawatt laser. We show that the x-ray measurements provide information about the dynamics of the laser-plasma acceleration. For moderately relativistic pulses, the x-ray radiation indicates a small betatron amplitude, which correlates with non-Maxwellian electron spectra and modulated transmitted optical spectra, all indicative of wakefield acceleration of the electrons. For increased laser intensity stronger x-ray emission indicates a larger betatron amplitude. In this case, electron energy gain is mainly due to a betatron resonance with the laser field, which serves to thermalize the electron spectra. Large amplitude transverse oscillations give rise to an x-ray beam that is well described in the synchrotron asymptotic limit.

The experiments were performed using the Vulcan Petawatt laser with central wavelength $\lambda_0 = 1.055\ \mu$m. The focusing geometry could be changed from $f/3$ to $f/5$ by reducing the beam diameter before focusing. This yielded a pulse length of $\tau_l = (630 \pm 120)$ fs and a near diffraction limited $1/e^2$ spot radius of $w_0 = 3.2\ \mu$m for the $f/3$. For the $f/5$, the corresponding values were $\tau_l = (760 \pm 120)$ fs and $w_0 = 5.3\ \mu$m. The laser was focused on the front edge of a supersonic gas jet with a plastic nozzle of diameter 1 to 5 mm. The maximum energy on target was 280 J for $f/3$ and 90 J for $f/5$. This yielded laser parameters $9 < a_0 < 29$, where $a_0 = 0.89 \times I^{1/2}[10^{18}\ \mathrm{W\,cm^{-2}}]\lambda_0\ [\mu\mathrm{m}]$, I is the peak focused intensity. Helium was used as a target gas and electron densities up to $n_e = 2n_i = 1.4 \times 10^{20}\ \mathrm{cm^{-3}}$ could be achieved, where n_i is the density in the ion channel.

A magnetic spectrometer measured electrons with energies from 20 to 200 MeV. X rays were measured with suitably filtered image plate detectors in the direct forward direction after the electrons had been deflected by the magnet. The image plates were absolutely calibrated [9]. Initially, a grid of wires was placed a few centimeters from the target. A radiograph consisting of the shadow of the grid was observed, indicative of a submillimeter source of x-ray radiation close to the laser focus.

To quantify the source dimensions more accurately, penumbral images were taken of a knife-edge. The $1/e$ x-ray source size is found to increase almost linearly with plasma density in both the horizontal and vertical directions, consistent with enhanced laser filamentation at high densities. For $n_e = 1.6 \times 10^{19}\ \mathrm{cm^{-3}}$, we find a $1/e$ source size of 90 μm; for $n_e = 1.4 \times 10^{20}\ \mathrm{cm^{-3}}$, it is 250 μm. Varying the interaction length by changing the nozzle length at constant density did not affect the x-ray source size appreciably. Replacing the plastic nozzle with a high Z brass nozzle indicates that the contribution of bremsstrahlung from the nozzle is negligible.

X-ray yields were measured through various metal foils with $1/e$ cutoff energy ranging from keV to tens of keV. Foils were chosen with identical transmission characteristics except for a narrow energy range around their K edges to create a pair of differential filters, usually called Ross filters. From the measurements, the total number of photons per steradian per energy bin can be deduced. By using a number of filters, a spectrum of the x rays could be constructed. This was measured simultaneously with the spectrum of relativistic electrons.

By changing the laser energy on target, an intensity scan was carried out for a 2 mm nozzle for $n_e = (1.6 \pm 0.2) \times 10^{19}\ \mathrm{cm^{-3}}$. Two markedly different types of electron spectra were observed [Fig. 1(a)]. At moderate $a_0 = 13$, the spectrum is clearly non-Maxwellian. Non-Maxwellian spectra are regularly observed in (self-modulated) laser wakefield acceleration (LWFA) [10]. At high $a_0 = 20$, 25, 27, the spectra become more Maxwellian, with a steadily increasing effective temperature T_{eff} for increasing a_0. The thermalization could be due to phase rotation of electrons once they became dephased in a plasma wave, but is also a characteristic of direct laser acceleration (DLA) [7,11]. The variation of maximum electron energy and temperature T_{eff} with increasing a_0 though is strongly indicative of DLA.

The simultaneously measured x-ray radiation emitted directly forward was found to increase with laser intensity, for a set of filters (5 μm Al, 20 μm Ni, 1.5 mm Al) with different cutoff energies (1.2 keV, 7 keV, 22 keV). In Fig. 1(b), the photon yield per solid angle through a 20 μm Ni filter is plotted. For this case, the x-ray yield can be easily compared with that predicted by the SAL. Equation (2) reduces to $N_{\mathrm{ph}} \propto N_e r_\beta$, since the plasma density is constant, and the number of betatron oscillations for a constant interaction length scales as $N_\beta \propto \lambda_\beta^{-1} \propto n_e^{1/2}\gamma_{z0}^{-1/2}$, with $\lambda_\beta = 2\pi c/\omega_\beta$. The electron number N_e was measured. N_{ph}/N_e, which is proportional to the betatron oscillation amplitude r_β, is also plotted in Fig. 1(b). This ratio and therefore r_β increases dramatically, by over 1 order of magnitude, from the lowest a_0 to higher a_0. It would be thought that if electrons were wakefield accelerated, the amplitude r_β would not depend strongly on a_0.

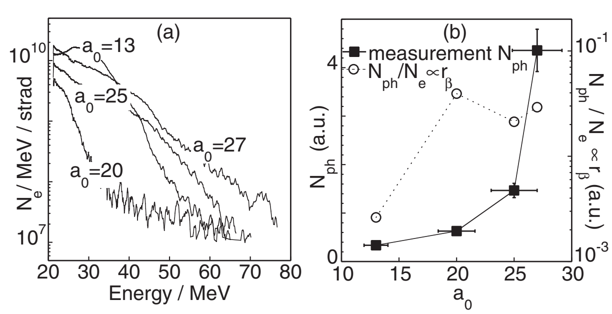

FIG. 1. (a) Electron energy distribution and (b) x-ray photon yield N_{ph} (solid square) and N_{ph}/N_e (open circle) for different a_0 with $f/3$ focusing, $D = 2$ mm, and $n_e = 1.6 \times 10^{19}\ \mathrm{cm^{-3}}$.

The observed increase in betatron amplitude r_β correlated with the change in the electron spectra strongly suggests a transition to a regime where electrons are accelerated by DLA. In this scenario, the higher laser intensities drive larger transverse oscillations [7]. For moderate a_0, the acceleration is mostly axial (i.e., r_β is small) and the radiation per electron due to transverse oscillations in the channel is negligible. This indicates that the acceleration at moderate a_0 is mostly wakefield driven.

This transition from wakefield dominated to DLA dominated acceleration is also indicated by analysis of the transmitted laser spectra. The spectra are more severely modulated at moderate intensity than for the higher intensities, as has been observed previously [12]. Cavitation due to increasing a_0 serves to inhibit Raman processes while enhancing DLA [6].

Figure 2(a) plots the x-ray signal through a 20 μm Ni filter for a scan of density conducted with a 5 mm nozzle for $a_0 = 10$. Below a certain density, the x-ray yield vanishes rapidly. For increased densities, the x-ray signal stays high and drops slowly. A similar trend was observed for the other filters. The density scaling is fundamentally different from other radiation mechanisms such as bremsstrahlung or nonlinear Thomson scattering. The former scales $\propto n_e^2$ when observed on axis and the latter $\propto n_e$ [5]. A comparable scaling of the x-ray intensity with plasma density was obtained from LWFA and was attributed to synchrotron radiation from electrons undergoing betatron oscillations in the plasma wake [3]. In our case, SAL [Eq. (2)] reduces to $N_{\mathrm{ph}} \propto N_e n_e r_\beta$. N_e and n_e have been measured. The scaling of r_β with density is not immediately clear. An upper limit for r_β is the size of the plasma channel, which decreases with density. However, DLA will dominate over LWFA at higher densities [13], and resonant coupling between the laser and the transverse oscillations may lead to an effective increase of r_β with density. Assuming r_β is constant, the SAL estimate using the measurement for N_e and n_e fits the measured x-ray yields well [Fig. 2(a)]. The discrepancy between fit and data suggests an increase of r_β with density.

Changing the interaction length was investigated by varying the nozzle diameter D from 1 to 5 mm in steps of 1 mm, with all other parameters constant. The electron spectra exhibit two markedly different shapes, similar to those plotted in Fig. 1(a). For $D = 1$ and 2 mm nozzles, the distribution is non-Maxwellian. An increase to $D = 3$ and 5 mm yields increasingly Maxwellian spectra. Consistent with previous studies [6], this demonstrates that for efficient DLA some preacceleration by LWFA is required. The x-ray yield is found to increase almost linearly with D [Fig. 2(b)], consistent with the anticipated scaling of yield in the SAL due to a linear increase in N_β.

To obtain a spectrum of the x rays, up to six filters were used simultaneously per shot with $1/e$ cutoff energies from keV to tens of keV allowing for a reliable reconstruction of the critical energy E_{crit}. In the SAL the spectrum can be approximated by a generalized form of Eq. (1). Convolving the spectrum with the filter transmission $T(E)$ and the image plate response $R(E)$, the x-ray energy deposition P can be calculated for each filter i and proportionality factor α, $\int \frac{d^2I}{dEd\Omega} T_i(E)R(E)dE = \alpha P_{\mathrm{calc},i}$. Minimizing $\chi^2 = \sum_i(\alpha P_{\mathrm{calc},i} - P_{\mathrm{meas},i})^2$ yields the best fit parameter E_{crit}. Figure 3(a) shows an example of a least squares fit giving $E_{\mathrm{crit}} = 20$ keV. The critical energy of the synchrotron spectrum E_{crit} decreases with plasma density [Fig. 3(b)] and increases with nozzle length. The maximum electron energy and effective Maxwellian temperature T_{eff} of the electron distribution are also found to decrease with density [Fig. 3(b)].

In the case of a monoenergetic electron beam, $E_{\mathrm{crit}} = 3\hbar\gamma_{z0}^2\omega_p^2 r_\beta/2c$. Even for electron beams with a broad spectrum, not all electrons contribute to the radiation equally. Low energy electrons are more abundant, but high energy electrons will radiate γ_{z0}^4 times more energy per solid angle. Considering, for example, the shot at 1.6×10^{19} cm^{-3} with $E_{\mathrm{crit}} = 29$ keV from Fig. 3(b), the product of these two effects is maximized for electrons with $60 < \gamma_{z0} < 80$. Hence, $r_\beta = (30 \pm 10)$ μm can be estimated. Previously, oscillation amplitudes of $r_\beta \cong 2$ μm have

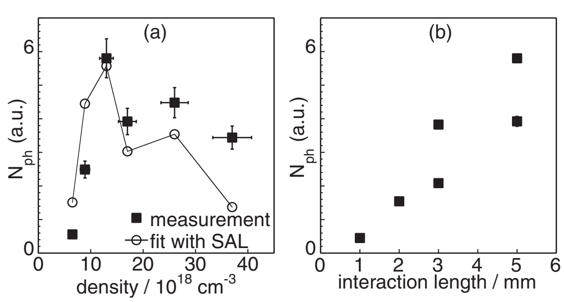

FIG. 2. X-ray photon signal as a function of plasma density (a) and interaction length D (b) for $f/5$ focusing and $a_0 = 10$.

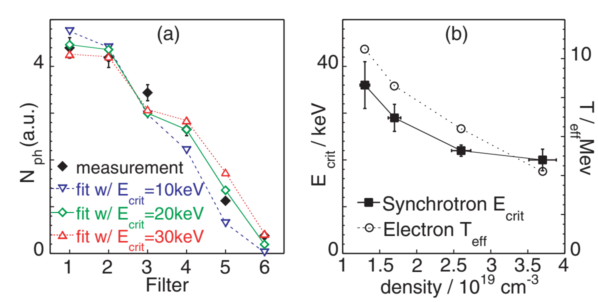

FIG. 3 (color online). (a) Measured and modeled x-ray signal for different filters for $n_e = 3.7 \times 10^{19}$ cm^{-3}. The filters, from left to right, are V 20 μm, Ti 30 μm, Ni 20 μm, Fe 30 μm, Al 1.5 mm, and Cu 270 μm. Modeling is based on a SAL spectrum with different E_{crit}. (b) Scaling of E_{crit} and T_{eff} with n_e. Shots were taken with $f/5$ focusing on a $D = 5$ mm nozzle at $a_0 = 10$.

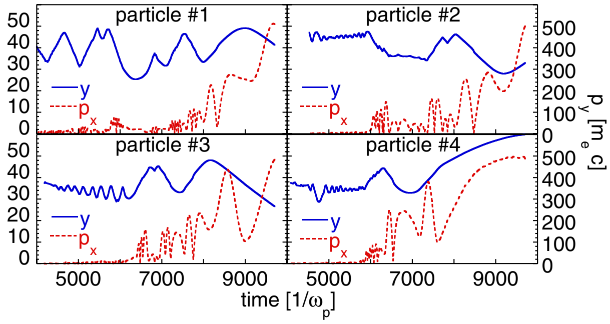

FIG. 4 (color online). Electron trajectories from simulation showing transverse deflection y and axial momentum p_x.

been reported in a LWFA regime [14]. An r_β of 30 μm corresponds to $a_\beta = \gamma_{z0} r_\beta k_\beta \cong 130 \gg 1$, which not only justifies the treatment of radiation in the framework of SAL but also represents the most violent optical plasma wiggler realized to date. With a_β and γ of order 100, the divergence angle of the radiation $\theta \sim a_\beta/\gamma \simeq 60°$ can be expected. This is consistent with a divergence angle of 50°–95°, which has been experimentally determined for comparable laser and target parameters [15].

Simulations with the particle-in-cell code OSIRIS were performed to study if and under what conditions such large oscillation amplitudes can occur. Trajectories of test electrons were tracked. All electrons exhibit oscillations across the channel, but the motion is not a simple betatron resonance oscillation. A set of sample trajectories is shown in Fig. 4. For most of the interaction, particles 2, 3, and 4 oscillate with small amplitudes on the order of several μm without picking up significant axial momentum. Any radiation produced in this preacceleration phase will add little to the measured x-ray yields. After a while, the oscillation amplitude starts to rise and suddenly increases to 10 μm. At the same time, the transverse electron energy is found to increase, indicative of a resonant coupling with the laser field. This transverse momentum is transferred to axial momentum via the $\mathbf{v} \times \mathbf{B}$ force. These particles perform only a few oscillations before they lose phase with the laser due to relativistic mass increase. Only particle 1 performs several oscillations with large amplitudes. For electrons that hit the betatron resonance, $r_\beta > 10$ μm is regularly observed and limited only by the channel diameter. This is in good agreement with the oscillation amplitude deduced from the electron and synchrotron spectra.

Making use of the x-ray measurements with differential filters, absolute photon numbers can be determined. Under optimum conditions, the total number of photons is found to be more than 5×10^8 ph/mrad^2/0.1% bandwidth (BW) in the spectral range from 7 keV to 12 keV where the typical electron charge is 2 nC for electrons with $40 < \gamma < 160$. This is about 10 times more photons per electron than previously achieved with a keV synchrotron source in a regime dominated by LWFA [16]. In our work, the electron acceleration is strongly influenced by the very high $a_0 > 10$. Direct laser acceleration, i.e., resonant driving of the transverse electron oscillations leads to an increase in the oscillation amplitude. This becomes manifest in the observed synchrotron spectra with E_{crit} as high as (36 ± 5) keV and divergence $\theta > 50°$. The x-ray beam typically contains a total energy of 2 mJ, i.e., $\sim 5 \times 10^{-2}$ of the total energy in the relativistic electrons or $\sim 5 \times 10^{-5}$ of the total energy in the laser pulse. Approximately 10% of the x-ray energy is emitted above 50 keV. The peak brightness of the x-ray beam is estimated from the pulse duration of the laser and the x-ray source size to be 1×10^{17} ph/s/mm^2/mrad^2/0.1% BW, similar to second generation wigglers. The amount of x-ray energy radiated per electron illustrates the problem of radiation damping, which will become more important at ultrahigh irradiance laser-plasma interactions [17].

In conclusion, we have demonstrated that electron acceleration in a DLA dominated regime produces a plasma wiggler with much higher strength parameter as compared to the wakefield regime. This leads to an x-ray source that extends to much higher energies than previously achieved while sharing the benefits of brightness, short pulse duration, and laser synchronization with other all optical synchrotron sources [14,16]. A hard x-ray synchrotron source could significantly expand the current scope of x-ray diffraction and absorption studies in ultrafast x-ray science.

The authors acknowledge the assistance of the staff of the Central Laser Facility at the Rutherford Appleton Laboratory. S. K. acknowledges the EUROLEAP network for financial assistance.

[1] N. Patel, Nature (London) **449**, 133 (2007).
[2] S. P. D. Mangles *et al.*, Nature (London) **431**, 535 (2004); J. Faure *et al.*, *ibid.* 431, 541 (2004); C. G. R. Geddes *et al.*, *ibid.* 431, 538 (2004).
[3] A. Rousse *et al.*, Phys. Rev. Lett. **93**, 135005 (2004).
[4] D. H. Whittum, A. M. Sessler, and J. M. Dawson, Phys. Rev. Lett. **64**, 2511 (1990).
[5] K. Ta Phuoc *et al.*, Phys. Rev. Lett. **91**, 195001 (2003).
[6] S. P. D. Mangles *et al.*, Phys. Rev. Lett. **94**, 245001 (2005).
[7] A. Pukhov *et al.*, Phys. Plasmas **6**, 2847 (1999).
[8] E. Esarey *et al.*, Phys. Rev. E **65**, 056505 (2002).
[9] S. G. Gales and C. D. Bentley, Rev. Sci. Instrum. **75**, 4001 (2004).
[10] B. Hidding *et al.*, Phys. Rev. Lett. **96**, 105004 (2006).
[11] G. D. Tsakiris *et al.*, Phys. Plasmas **7**, 3017 (2000).
[12] B. R. Walton *et al.*, Phys. Plasmas **13**, 113103 (2006).
[13] C. Gahn *et al.*, Phys. Rev. Lett. **83**, 4772 (1999).
[14] K. Ta Phuoc *et al.*, Phys. Rev. Lett. **97**, 225002 (2006).
[15] This measurement was performed in a later experiment on the Vulcan laser, fielding two x-ray detection channels at 0° and 45° from the laser axis.
[16] K. Ta Phuoc *et al.*, Phys. Plasmas **12**, 023101 (2005).
[17] J. Koga *et al.*, Phys. Plasmas **12**, 093106 (2005).